7. S. Hu, G. Yang, Y. Jing, C. Gao, G. Wei, and F. Lu, Stable ns pulses generation from cladding-pumped Yb-doped fiber laser, Microwave Opt Technol Lett 48 (2006), 2442–2444.

8. H. Lim, F.Ö. Ilday, and F.W. Wise, Generation of 2-nJ pulses from a femtosecond ytterbium fiber laser, Opt Lett 28 (2003), 660–662.

9. L. Ren, L. Chen, M. Zhang, C. Zhou, Y. Cai, and Z. Zhang, Group delay dispersion compensation in an Ytterbium-doped fiber laser using intracavity Gires–Tournois interferometers, Opt Laser Technol 42 (2010), 1077–1079.

10. H. Lim, F.O. Ilday, and F.W. Wise, Femtosecond ytterbium fiber laser with photonic crystal fiber for dispersion control, Opt Exp 10 (2002), 1497–1502.

11. G. Lin, S. Lee, G. Lin, and K. Lin, Picosecond chirped-pulse amplification in traveling-wave semiconductor optical amplifiers, Microwave Opt Technol Lett 33 (2002), 202–207.

12. H. Song, S.B. Cho, D.U. Kim, S. Jeong, and D.Y. Kim, Ultra-high-speed phase-sensitive optical coherence reflectometer with a stretched pulse supercontinuum source, Appl Opt 50 (2011), 4000–4004.

13. A. Chong, J. Buckley, W. Renninger, and F.W. Wise, All-normal-dispersion femtosecond fiber laser, Opt Exp 14 (2006), 10095–10100.

14. W.H. Renninger, A. Chong, and F.W. Wise, Dissipative solitons in normal-dispersion fiber lasers, Phys Rev A 77 (2008), 023814.

15. C. Le Blanc, P. Curley, and F. Salin, Gain-narrowing and gain-shifting of ultra-short pulses in Ti:sapphire amplifiers, Opt Commun 131 (1996), 391–398.

16. M.A. Larotonda, Saturation of Kerr-lens mode locking and the self-amplitude modulation coefficient, Opt Commun 228 (2003), 381–388.

17. H.A. Haus, Mode-locking of lasers, IEEE J Sel Top Quantum Electron 6 (2000), 1173–1185.

WIDEBAND MULTILAYER DIRECTIONAL COUPLER WITH TIGHT COUPLING AND HIGH DIRECTIVITY

Antonije R. Djordjević,[1] **Veljko M. Napijalo,**[2] **Dragan I. Olćan,**[1] **and Alenka G. Zajić**[3]
[1] School of Electrical Engineering, University of Belgrade, P.O. Box 35-54, 11120 Belgrade, Serbia; Corresponding author: olcan@etf.rs
[2] Independent Researcher, 6 Belvedere, Marine Drive, Paignton, Devon, TQ3 2NS, United Kingdom
[3] School of Computer Science, Georgia Institute of Technology, Atlanta GA 30332

ABSTRACT: *A novel, wideband, symmetrical, printed directional coupler is described, which has tight coupling and high directivity. The coupler consists of four interconnected strips printed in two layers. The dimensions of the strips are optimized to minimize the dispersion of propagating modes. Design data are provided for some typical practical cases. The theoretical results are verified experimentally.* © 2012 Wiley Periodicals, Inc. Microwave Opt Technol Lett 54:2261–2267, 2012; View this article online at wileyonlinelibrary.com. DOI 10.1002/mop.27051

1. INTRODUCTION

Multilayer techniques in fabrication of printed-circuit boards, ceramic devices, as well as thin- and thick-film technologies have enabled miniaturization and inexpensive mass production. These techniques also offer possibilities for designing new structures for microwave circuits, which may have better performance than classical circuits.

One group of such circuits consists of microstrip directional couplers with distributed coupling [1], which have gained significant interest in the literature for decades [2–17], even recently [18–21]. In this article, we consider microstrip structures, which are planar structures with a solid ground plane on the bottom face, are open on the top, have one or several dielectric layers whose permittivities may be different, and have strips, placed parallel to the ground, in any layer. The ground plane serves as the reference for all signals and also creates an electromagnetic shield toward any other components or objects that may be located underneath. We exclude from consideration other planar transmission lines, such as striplines, coplanar waveguides, and planar lines.

Microstrip structures have an inhomogeneous medium, because the air is always above the substrate. Hence, the waves that are guided by the microstrip structures are hybrid waves (quasi-TEM waves). In the general case, the hybrid waves exhibit dispersion at very high frequencies (intramodal dispersion). The intramodal dispersion is augmented by losses in conductors and dielectrics. Besides the intramodal dispersion, coupled microstrip lines suffer from the intermodal dispersion. i.e., the characteristic modes propagate at various velocities [22]. For two classical symmetrical coupled microstrip lines, the even mode (common mode) travels more slowly than the odd mode (differential mode). Although the difference in velocities is on the order of a few percent, the intermodal dispersion significantly deteriorates the isolation of coupled-line directional couplers, and, hence, deteriorates the directivity.

Various techniques have been implemented to reduce the effect of the intermodal dispersion. For example, the odd mode can be slowed-down by increasing the capacitive coupling between the traces using small dents (interdigital capacitors) along the lines. Alternatively, the effect of the different modal velocities can be compensated by lumped capacitances located at the ends of a directional coupler [16]. However, the compensation at the ends of the coupler results only in a relatively narrowband improvement of the directivity [23].

Instead of compensating the intermodal dispersion, several techniques have been published for obtaining microstrip structures that inherently have equalized modal velocities. For example, edge-coupled microstrip lines can be covered with a metallic shield at a height that is equal to the substrate thickness [24] or a dielectric overlay can be used [7]. Modal velocities can also be equalized by introducing a slit in the ground plane [8] or adding coupled strips on a vertical printed-circuit board [6]. In Ref. 5 several multilayer structures are described that have equalized velocities for two symmetrical coupled microstrips. However, the structures described in Ref. 5, 7, 8 are not suitable for tight coupling, and the structure from Ref. 6 may be complicated for manufacturing.

In Ref. 15 various multilayer structures with two and three strips are described that equalize the capacitive and inductive coupling and, consequently, equalize the modal velocities. The equalization is achieved by selecting the geometry parameters, as well as the relative permittivities of dielectric layers (i.e., an inhomogeneous dielectric is used). A good isolation was obtained in the experiments for hybrid couplers: about 30 dB in an octave bandwidth. However, certain restrictions to the range of dielectric permittivities apply in the designs. Furthermore, the structures do not have symmetrical/antisymmetrical modes and the ports are not symmetrically placed on the coupler. As the
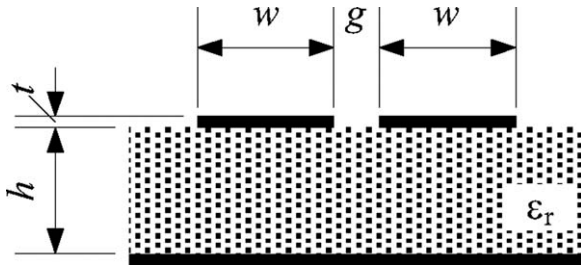
Figure 1 Edge-coupled microstrip lines

result, phase-compensating devices are required at the ports. Similarly, in Ref. 18, a three-strip multilayer coupler is presented with equalized capacitive and inductive coupling, and with compensated parasitic reactances between terminal lines and coupled lines. The obtained directivity is about 30 dB, but the coupler structure is also asymmetrical and phase compensating lines are required at the terminals.

Another problem with microstrip couplers occurs due to technological limitations. The separation between traces cannot be made too small, which restricts the coupling if the lines are located in a single layer (edge-coupled lines). The classical way to increase the coupling is to interleave several strips, leading to various versions of the Lange coupler [2]. These strips, however, require interconnections (bridges) at several places. The classical technique is to bond small wires, which can be considered as a rudimentary multilayer technique. The modern approach is to use the advantages of the multilayer processing and make the bridges by traces printed on adjacent layers [9, 20]. The Lange couplers enable production of hybrid couplers (3 dB couplers), though, in some cases, more than four strips must be interleaved [3, 17] or classical Lange couplers should be cascaded [4]. Besides providing strong coupling, the Lange couplers are known to reduce the intermodal dispersion (but not completely eliminate it) and, hence, provide a good directivity. However, the Lange couplers do not take full advantage of multilayer processing because the strips are located only in one layer and they occupy a relatively large footprint area. In addition, the Lange couplers do not possess symmetry.

Smaller footprint area and strong coupling are achievable if two strips are printed on different layers, on top of each other (broadside-coupled lines), e.g., Ref. 10, 11, 15, 19. The broadside-coupled lines can provide overcoupling (coupling stronger than 3 dB), which is required for broadband hybrids. However, due to the dielectric inhomogeneities, the intermodal dispersion is pronounced, which deteriorates the coupler directivity. In addition, the broadside-coupled lines do not support symmetrical modes.

The need for having a symmetrical structure was the motive in Ref. 14 to use a four-strip structure in two layers, where diagonally opposite strips are interconnected at the terminals of the coupler. In the design, the authors selected equal gap widths in both layers. However, unfortunately, the authors did not recognize the full potential of this structure—that the modal velocities can be equalized—and the isolation reported in Ref. 14 is only about 16 dB. However, a good phase tracking between the ports is shown.

To address all the deficiencies of the existing microstrip structures, mentioned above, we start from a structure similar to the one in Ref. 14 and design a family of symmetrical compact multilayered transmission-line structures, which inherently have equalized modal velocities and which can be used for production

of high-performance directional broadband couplers with tight coupling and a small footprint.

The rest of the article is organized as follows. The novel structure is presented in Section "A New Multilayer Microstrip Structure with Equalized Modal Propagation Velocities". In Section "High-Performance Hybrid Coupler", using the new structure, an octave hybrid directional coupler is designed and computed and measured scattering parameters are presented. Finally, in Section "Conclusions," possibilities and limitations of the proposed structure are discussed.

2. A NEW MULTILAYER MICROSTRIP STRUCTURE WITH EQUALIZED MODAL PROPAGATION VELOCITIES

To introduce our new multilayer microstrip structure with equalized model propagation velocities, we first analyze the performance of the edge-coupled and broadside-coupled microstrip lines.

First, we consider two symmetrical "edge-coupled" microstrip lines, shown in Figure 1. As a numerical example, let the substrate thickness be $h = 1$ mm, relative permittivity $\varepsilon_r = 4.5$, strip width $w = 1.4$ mm, gap (separation) width $g = 0.2$ mm, and metallization thickness $t = 36$ μm. In this section, we neglect conductor and dielectric losses.

Such coupled lines can be analyzed based on the theory of modes [22]. We analyze this multiconductor system by a quasi-static approach [24]. Two modes can propagate along this symmetrical structure: the even mode and the odd mode. The velocity of the odd mode ($v_o \approx 180$ Mm/s) is higher than the velocity of the even mode ($v_e \approx 160$ Mm/s). This can be explained as follows. For the odd mode, the strips are at the opposite potentials. Hence, there is a strong electric field in the gap and its vicinity, and a significant fraction the electric field energy is located in the air. For the even mode, the conductors are at the same potential, and the electric field in the gap and its vicinity is practically negligible. Hence, the odd mode has relatively more electric energy in the air than has the even mode, so that the odd mode travels faster.

These coupled lines constitute a directional coupler, whose coupling is 9.4 dB and the directivity is only about 11.3 dB. (In all examples in this article, the nominal port impedance is 50 Ω.) For comparison, a four-strip Lange coupler on the same substrate, with $w = 0.35$ mm and $g = 0.2$ mm, has a stronger coupling (4.5 dB), and a better directivity (about 19 dB).

Then, we consider the "broadside-coupled" lines shown in Figure 2. When the two strips are driven in counter-phase, there exists a strong electric field in the space between the strips. Hence, a lot of electric energy is located in this space. However, the structure does not have a proper plane of symmetry, so that
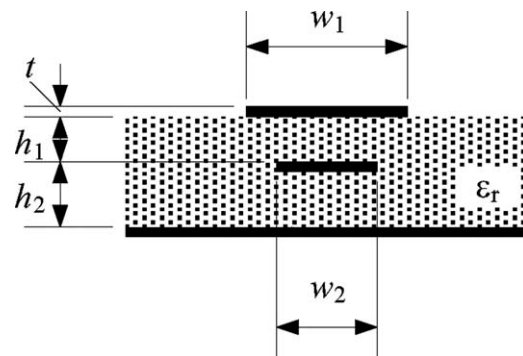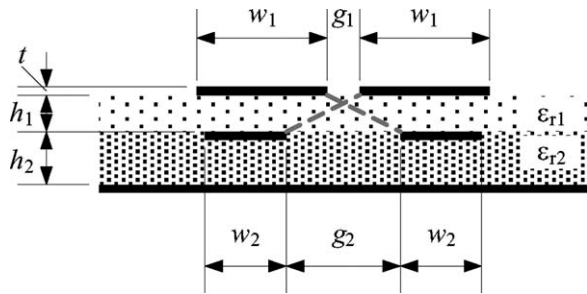

Figure 2 Broadside-coupled lines

Figure 3 Proposed multiconductor transmission-line structure with equalized modal velocities

the two characteristic modes do not even resemble an even mode or an odd mode. For each mode, the conductor potentials have the same sign, whereas the currents are oppositely directed. The potential of one strip is several times larger than the potential of the other strip. One strip serves almost like a part of the ground conductor for the other strip. As an example, for $h_1 = 0.5$ mm, $h_2 = 0.5$ mm, $\varepsilon_r = 4.5$, $w_1 = 1.5$ mm, and $w_2 = 0.58$ mm, a directional coupler is obtained whose coupling is 6.6 dB and the directivity is 21 dB. Obviously, the directivity is better than for the edge-coupled microstrips. The velocity of the modes are $v_1 \approx 165$ Mm/s and $v_2 \approx 140$ Mm/s. The performance of this coupler can be improved in the vicinity of the central frequency by placing lumped capacitances between the terminals and the ground, as in Ref. 16.

To obtain inherently equalized model propagation velocities, we propose to combine the structures shown in Figures 1 and 2. The cross section of the novel coupler, proposed in this article, is shown in Figure 3. The structure consists of four strips: two are printed on the top metallization layer, and two on the intermediate metallization layer. The diagonally located strips are mutually interconnected. A ground plane is located at the bottom metallization layer. The relative permittivities of the two layers (ε_{r1} and ε_{r2}) can be arbitrary and the substrate can have more layers than shown. However, in all examples in this article, we take two layers with $\varepsilon_{r1} = \varepsilon_{r2} = \varepsilon_r$.

In a simplified view, each pair of strips in Figure 3 is coupled in two ways. The first way is similar to the edge coupling between a microstrip pair shown in Figure 1. This mechanism results in a faster propagation of the odd mode. The second way of coupling is similar to the broadside coupling between the two strips shown in Figure 2 and it results in a faster propagation of the even mode. By balancing the two coupling mechanisms, the velocities of modal propagation can be equalized. In reality, the equalization of the propagation coefficients is not perfect because the attenuation coefficients of the two modes are different.

If we assume that the interconnections in Figure 3 are ideal, i.e., they introduce no parasitic reactances, and that they are distributed densely all along the multiconductor structure, each pair of mutually interconnected strips can be rigorously treated as a single "logical" conductor. The resulting structure is symmetrical, which is usually a desirable feature for directional couplers, and it supports two modes: the even mode and the odd mode. The coupling between the two "logical" conductors is a combination of the edge coupling between the two strips on the top face of the substrate, the edge coupling between the two strips buried in the dielectric, and the broadside coupling between the pairs of vertically aligned strips. The equalization of the modal velocities is obtained in a wide frequency range, up to very high frequencies where the intramodal dispersion becomes significant.

Directional couplers can be designed based on the proposed structure, using an optimization of the cross-sectional dimensions. In addition to equalizing the modal velocities, the optimization should yield a proper characteristic impedance matrix of the multiconductor structure, which is necessary to design a well-matched directional coupler with a given coupling. For example, a coupling of 6.1 dB at the central frequency is achieved for $h_1 = 0.5$ mm, $h_2 = 0.5$ mm, $\varepsilon_r = 4.5$, $w_1 = 0.24$ mm, $w_2 = 0.17$ mm, $s_1 = 0.70$ mm, $s_2 = 0.48$ mm, and $t = 36$ μm. The modal velocities are equal within the numerical error, i.e., $v_e = v_o = 156$ Mm/s. The isolation, theoretically, attains infinity, whereas numerical simulations using program [24] show an isolation of about 80 dB.

Besides providing an excellent equalization, the multiconductor structure shown in Figure 3 enables obtaining a strong coupling between the two "logical" conductors. Achievable coupling levels depend on the printing resolution and on the ratio h_1/h_2. To obtain a coupling stronger than about 5 dB, the ratio h_1/h_2 should be smaller than 1, i.e., the upper dielectric layer should be thinner than the lower layer. As an example, for $\varepsilon_r = 4.5$, $h_1 = 0.4$ mm, and $h_2 = 1.6$ mm, Table 1 gives the optimized dimensions versus the required coupling (C) at the central frequency. The printing resolution is assumed to be 0.01 mm and the conductor thickness is $t = 36$ μm. The narrowest gap and strip are taken to be 0.2 mm. It is also assumed that $w_1 = w_2$. The results are obtained using the optimization in program [25]. The optimization function is multimodal. Hence, there exists a multitude of solutions for the given criteria. For example, for the coupling of 3 dB, an alternative optimal solution is $w_1 = 0.27$ mm, $w_2 = 0.58$ mm, $g_1 = 0.45$ mm, and $g_2 = 0.56$ mm.

To a certain extent, the proposed structure resembles a Lange coupler because it has four strips, two and two being mutually interconnected. However, in a classical Lange coupler, all strips are in the same layer and edge-coupled, whereas in the proposed structure, the strips are in different layers and have a combined coupling. Compared with a Lange coupler, the proposed structure allows for a stronger coupling and also for a much better equalization of the modal velocities. In addition, the proposed structure is almost perfectly symmetrical, unlike the Lange coupler.

3. HIGH-PERFORMANCE HYBRID COUPLER

To verify the proposed concept, we design a directional coupler based on the structure shown in Figure 3, for the octave bandwidth from 0.165 GHz to 0.335 GHz, on an inexpensive substrate (FR-4) and using classical printing technology. In the computer simulations presented in this section, we take into account losses in the conductors and in the dielectric [26, 27].

As we require a strong coupling, first we have to appropriately select the ratio h_1/h_2. Thereafter, we have to optimize the

TABLE 1 Design Data for Various Coupling Levels

C (dB)	$w_1 = w_2$ (mm)	g_1 (mm)	g_2 (mm)
5	0.33	3.50	4.20
4.5	0.35	2.30	2.94
4	0.38	1.39	2.04
3.5	0.41	0.77	1.40
3	0.42	0.41	0.93
2.5	0.40	0.20	0.52

Strip widths and separations are shown in Figure 3. Other data are given in the text.
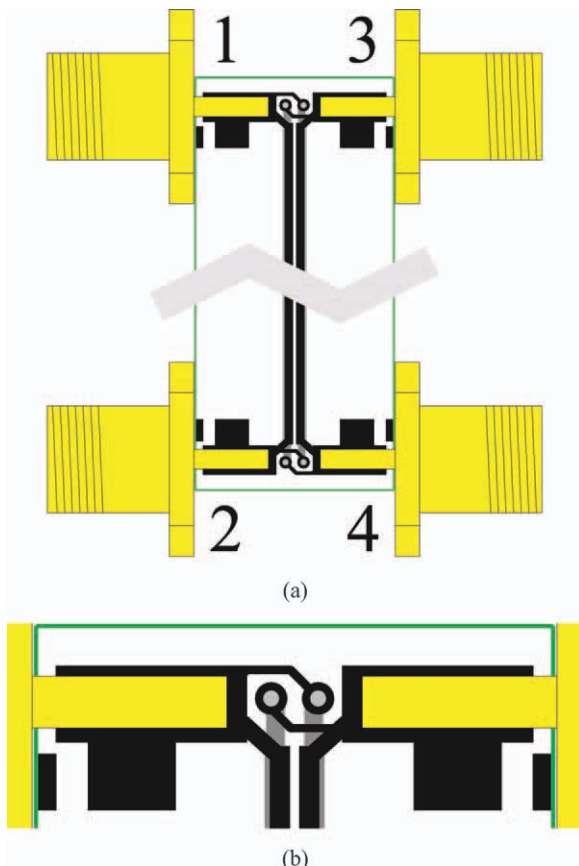
Figure 4 (a) PCB with SMA connectors. Black: top layer. Grey: intermediate layer. White: ground plane (bottom layer). (b) Zoom-in of the interconnections. [Color figure can be viewed in the online issue, which is available at wileyonlinelibrary.com]

strip widths and gaps to obtain the required coupling and maximize the isolation. The length of the coupled structure is determined by the central frequency of the coupler. As a broadband performance is required, the coupler should be overcoupled at the central frequency.

In practice, the interconnections shown in Figure 3 can be located only at a few places along the line. The most suitable locations are the beginning and the end of the coupled structure (Fig. 4), because at these ends, the terminals of the coupler have to be produced anyway. Consequently, we select to have the interconnections only at the two ends of the coupler. Due to the specific geometry, the interconnections are not perfectly symmetrical. However, for the particular substrate, frequency range, and technology, this imperfection is practically negligible.

Strictly speaking, having interconnections only at two places, invalidates the assumption of having only two "logical" conductors. In a rigorous analysis, the coupler must be treated as a multiconductor transmission line [22, 24, 25].

The multiconductor structure shown in Figure 4 supports four quasi-TEM modes. More precisely, it supports a total of eight waves: the incident and the reflected wave for each of the four modes. The four modes possess symmetry and antisymmetry with respect to the vertical plane, because the structure is symmetrical. However, their propagation velocities range from about 140 Mm/s to 180 Mm/s for the concrete dimensions of the structure described later in this section. Due to the presence of the four modes, and not only two, the reasoning from Section

"A New Multilayer Microstrip Structure with Equalized Modal Propagation Velocities" should be questioned.

Here, we note that at the central frequency of the coupler, the length of the coupled structure is quarter-wavelength. Even for a broadband coupler (e.g., an octave coupler), this length is safely below half-wavelength in the whole operating band. Under these conditions, we show that the analyzed structure can be approximately treated as if each pair of interconnected conductors represents one "logical" conductor, as assumed in Section "A New Multilayer Microstrip Structure with Equalized Modal Propagation Velocities.". The verification is carried out by simulations which show that the model involving two modes and the model involving four modes yield very similar scattering parameters in the whole frequency band of operation of the directional coupler considered (Fig. 5). The differences are primarily seen in the scattering parameters that have very low magnitudes. For example, the discrepancies between the two models are about 2 dB at the −40 dB level in the middle of the passband. Hence, the reasoning from Section "A New Multilayer Microstrip Structure with Equalized Modal Propagation Velocities" can be applied with sufficient reliability to the whole operating band of the coupler.

The discrepancies between the two models, however, become significant in the vicinity of the resonant frequencies (i.e., outside the operating band), when the coupler's length approaches an integer multiple of half-wavelength. At these frequencies, a pair of mutually interconnected strips behaves as resonator, short circuited at both ends. If for some practical reason these resonances are to be pushed towards higher frequencies, additional interconnections must be made at several locations along the coupled lines. Note that a similar reasoning regarding the number of modes and resonances also applies to the Lange couplers.

The substrate selected for the prototype is FR-4, whose relative permittivity is $\varepsilon_r = 4.5$ and the loss tangent is $\tan \delta = 0.025$ [27]. The strips are printed on the upper substrate (double-sided printing). The lower substrate carries the ground plane on the bottom face and it is void of copper on the upper face. The two substrates are joined by epoxy glue. The interconnecting vias are made on the upper substrate, resulting in blind vias. The conductor is copper and its thickness is $t = 36$ μm. To achieve a tight coupling required for a hybrid coupler, we take a thicker lower substrate ($h_2 = 1.61$ mm, which includes the glue
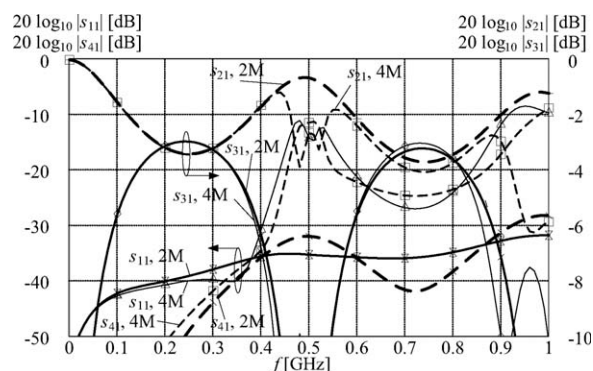
Figure 5 Scattering parameters of a hybrid coupler obtained by simulations [24] when the structure is considered to support 2 modes (2M) and 4 modes (4M). The left ordinate is for reflection (s_{11}) and isolation (s_{41}). The right ordinate is for transmission (s_{21}) and coupling (s_{31}). The numbering of ports is shown in Figure 4a
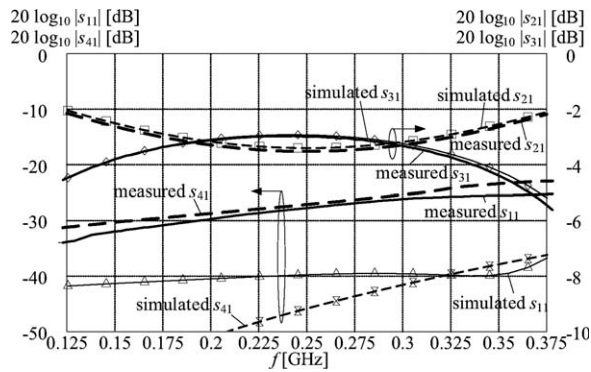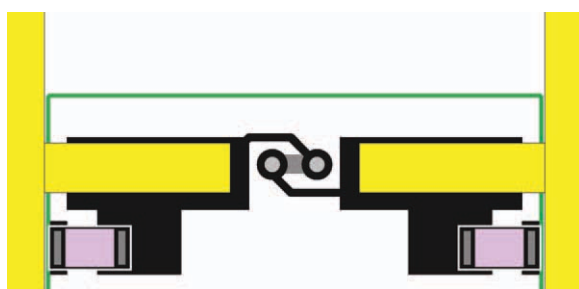
Figure 6 Scattering parameters of a hybrid coupler obtained by simulations [25] and measurements without compensating capacitances. The left ordinate is for reflection (s_{11}) and isolation (s_{41}). The right ordinate is for transmission (s_{21}) and coupling (s_{31}). The numbering of ports is shown in Figure 4a

Figure 8 Scattering parameters of a hybrid coupler obtained by simulations [25] and measurements with compensating capacitances. The left ordinate is for reflection (s_{11}) and isolation (s_{41}). The right ordinate is for transmission (s_{21}) and coupling (s_{31}). The numbering of ports is shown in Figure 4a

thickness) than the upper substrate ($h_1 = 0.5$ mm). The optimal dimensions of the coupler cross-section are $w_1 = w_2 = 0.46$ mm, $g_1 = 0.26$ mm, and $g_2 = 0.50$ mm. The length of the coupled lines is 160 mm.
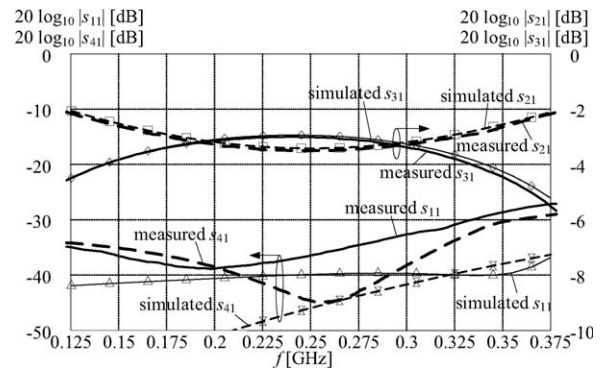
At the ends of the coupler, interconnections are made and four SMA connectors are mounted, as sketched in Figure 4. In the first cut of the design, the parasitic effects of the interconnections and connectors were not included. The rationale is that the zones that contain the interconnections and connectors are quasistatic, so that simple compensation of the discontinuities could be designed afterward. Figure 6 shows the scattering parameters of the coupler computed by modeling only the multiconductor transmission line, along with the measured scattering parameters of the prototype without compensating capacitors. In the measurements, performed using the network analyzer Agilent E5062A, the reference planes were positioned at the flanges of the SMA connectors.

The experiment showed that the discontinuities are predominantly inductive, so that capacitive compensations to ground, at the connectors, sufficed. As the interconnecting region is very small in terms of the wavelength, the capacitors simultaneously compensate all the inductances caused by the vias, the narrow and wider printed interconnection traces, and the transitions to the SMA connectors, which is the same strategy as in Ref. 18. Note that the width of a 50 Ω microstrip line (4 mm) is larger than the width of any printed trace in Figure 4.

The required compensations were determined in two ways. The first way was to measure the scattering parameters of the uncompensated coupler and then design the compensations in

program [25]. Thus, the best coupler directivity and the return loss were obtained for the compensating capacitances of 1.12 pF.

The second way of designing the compensating capacitances was to remove the coupled lines and directly interconnect two SMA connectors, as shown in Figure 7. Before the SMD compensating capacitors were mounted, the measured reflection coefficient at a port was −21.3 dB at 0.25 GHz, corresponding to an excess inductance of 5.5 nH. Thereafter, two identical SMA capacitors (1.2 pF each) were soldered as shown in Figure 7. The resulting reflection coefficient improved to −43 dB, which was considered to be sufficient for our purposes.
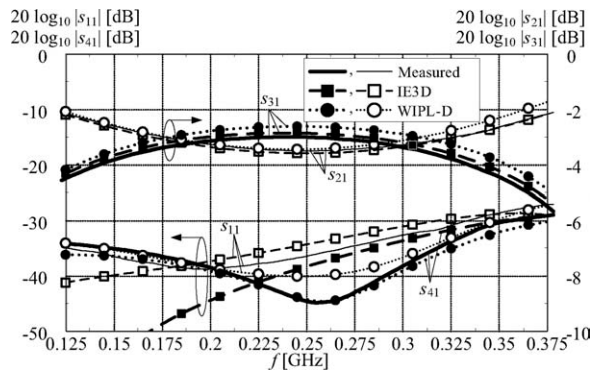
Figure 8 shows the measured scattering parameters of the prototype with compensating capacitors, along with the parameters computed by program [25]. Note that the declared reflection of the matched loads (used as calibration standards and also used to terminate the unused ports in measurements) is −46 dB. Taking into account the intrinsic reflections of the SMA connectors, one should be aware that the measured results below about −40 dB are not reliable. Hence, the quality of agreement between the simulated and measured results can be described as very good.

Further computer simulations of the prototype were carried out using programs IE3D [28] and WIPL-D [29]. IE3D assumes infinite dielectric layers with finite dielectric thickness. WIPL-D takes into the account all discontinuities in a fully 3D electromagnetic model. Both models include very detailed meshing of the interconnection area.

Figure 9 presents the simulation results along with the measured data, all of them with compensating capacitances. The compensating capacitances are 1.3 pF in the IE3D model, and 0.96 pF in the WIPL-D model. The capacitances differ because the port models in the two programs are different. A very good agreement is obtained between the three sets of results, thus confirming the proposed concept.

4. CONCLUSIONS

A novel multilayer, symmetrical, printed directional coupler is proposed, which consists of four interconnected strips located above a ground plane. The coupler inherently exhibits low dispersion in a wide frequency range, which is convenient for manufacturing directional couplers with tight coupling and high isolation (and, hence, with high directivity). The production requires multilayer technology, including manufacturing of blind

Figure 7 PCB without coupled lines: zoom-in of the interconnections and compensating capacitors. [Color figure can be viewed in the online issue, which is available at wileyonlinelibrary.com]

Figure 9 Scattering parameters of a hybrid coupler obtained by simulations [28], [29] and measurements with compensating capacitances. The left ordinate is for reflection (s_{11}) and isolation (s_{41}). The right ordinate is for transmission (s_{21}) and coupling (s_{31}). The numbering of ports is shown in Figure 4a

vias. Hence, the proposed structure is convenient for LTCC, MMIC, and thin-film productions.

To illustrate the performance of the proposed hybrid directional coupler, we have designed a hybrid coupler for the octave bandwidth from 0.165 GHz to 0.335 GHz, on an inexpensive substrate (FR-4). Very good agreement was obtained between 2D and 3D numerical simulations and measured data. The results demonstrate very good performance: mean coupling of 3.2 dB, return loss better than 30 dB, and isolation better than 32 dB. The directivity of the coupler is excellent: it is better than about 30 dB in practically the whole frequency range, and it is better than 40 dB around the central frequency.

The prototype produced on a relatively lossy substrate (FR-4) demonstrates that the performance of the coupler is not significantly degraded by the losses.

The proposed coupler can yield excellent directivity and tight coupling (2–10 dB). However, different layer thicknesses may be required to achieve this goal.

If the length of the coupled structure does not exceed, approximately, 40% of the wavelength, it is sufficient to have interconnections only at the terminals. If operation at higher frequencies is required, the interconnections may need to be also placed at several locations along the coupler.

The coupler ports can be in various orders, depending on how the port interconnections are made (on the top layer or on the bottom layer). This feature enables easy swapping of the ports, according to layout needs governed by neighboring microwave circuits.

The proposed directional coupler is inherently a 90°-coupler. For the designed and fabricated hybrid coupler, the measured deviation from the 90° phase shift is less than 2° in the whole operating band.

The coupler is compact. For the same substrate as described in Section "High-Performance Hybrid Coupler," the overall length is slightly longer than for a broadside-coupled hybrid (for 4%) and slightly shorter than for a Lange coupler with four strips (for 10%). The width of the metallization footprint is about 20% narrower than for the broadside-coupled hybrid and almost two times narrower than for the Lange coupler.

ACKNOWLEDGMENTS

REFERENCES

1. D. M. Pozar, Microwave engineering, 3rd ed., Wiley, New Jersey, 2005, pp. 337–352.
2. J. Lange, Interdigitated stripline quadrature hybrid, IEEE Trans Microwave Theory Tech 17 (1969), 1150–1151.
3. Y. Tajima and S. Kasmihashi, Multiconductor coupler, IEEE Trans Microwave Theory Tech 26 (1978), 795–801.
4. G. Kemp, J. Hobdell, and J. W. Biggin, Ultra-wideband quadrature coupler, Electron Lett 19 (1983), 197–199.
5. M. Horno and F. Medina, Multilayer planar structures for high-directivity directional coupler design, IEEE Trans Microwave Theory Tech 34 (1986), 1442–1449.
6. Y. Konishi, I. Awai, Y. Fukuoka, and M. Nakajima, A directional coupler of a vertically installed planar circuit structure, IEEE Trans Microwave Theory Tech 36 (1988), 1057–1063.
7. J.L. Klein and K. Chang, Optimum dielectric overlay thickness for equal even and odd-mode phase velocities in coupled microstrip circuits, Electron Lett 26 (1990), 274–276.
8. F. Masot, F Medina, and M. Horno, Theoretical and experimental study of modified coupled strip coupler, Electron Lett 28 (1992), 347–348.
9. D. Bourreau, B. Delia, E. Daniel, C. Person, and S. Toutain, High performance Lange coupler, Electron Lett 28 (1992), 1997–1998.
10. I. Toyoda, T. Hirota, T. Hiraoka, and T. Tokumitsu, Multilayer MMIC branch-line coupler and broadside coupler, IEEE MTT-S Int Microwave Symp Dig, Albuquerque, NM, 1992, pp. 79–82.
11. M.D. Prouty and S.E. Schwartz, Hybrid couplers in bilevel microstrip, IEEE Trans Microwave Theory Tech 41 (1993), 1939–1944.
12. C. Person, J. P. Coupez, S. Toutain, and M. Morvan, Wideband 3dB/90 coupler in multilayer thick-film technology, Electron Lett 31 (1995), 812–813.
13. S. Banba and H. Ogawa, Multilayer MMIC directional couplers using thin dielectric layers, IEEE Trans Microwave Theory Tech 43 (1995), 1270–1275.
14. H. Okazaki and T. Hirota, Multilayer MMIC broad-side coupler with a symmetric structure, IEEE Microwave Guided Wave Lett 7 (1997), 145–146.
15. K. Sachse and A. Sawicki, Quasi-ideal multilayer two- and three-strip directional couplers for monolithic and hybrid MIC's, IEEE Trans Microwave Theory Tech 47 (1999), 1873–1882.
16. S. Al-taei, P. Lane, and G. Passiopoulos, Design of high directivity directional couplers in multilayer ceramic technologies, IEEE MTT-S Int Microwave Symp Dig, Phoenix, AZ, 2001, pp. 51–54.
17. I. J. Bahl, Six-finger Lange coupler on 3mil GaAs substrate using multilayer MMIC technology, Microwave Opt Tech Lett 30 (2001), 322–327.
18. S. Gruszczynski, K. Wincza, and K. Sachse, Design of high performance three-strip 3-dB directional coupler in multilayer technology with compensated parasitic reactances, Microwave Opt Tech Lett 49 (2007), 1656–1659.
19. V. Napijalo and B. Kearns, Multilayer 180° coupled line hybrid coupler, IEEE Trans Microwave Theory Tech 56 (2008), 2525–2535.
20. A. Bikiny, C. Quendo, E. Rius, J.-F. Favennec, C. Person, B. Potelon, L. Rigaudeau, P. Moroni, and J. L. Cazaux, Ka-band Lange coupler in multilayer thick-film technology, IEEE MTT-S Int Microwave Symp Dig, Boston, MA, 2009, pp. 1001–1004.
21. H.H. Ta and A.-V. Pham, Development of a compact broadband folded hybrid coupler on multilayer organic substrate, IEEE Microwave Wireless Compon Lett 20 (2010), 76–78.
22. A.R. Djordjević, T. K. Sarkar, and R. F. Harrington, Time-domain response of multiconductor transmission lines, Proc IEEE 75 (1987), 743–764.
23. A. Sawicki and K. Sachse, A novel directional coupler for PCB and LTCC applications, IEEE MTT-S Int Microwave Symp Dig, Seattle, WA, 2002, pp. 2225–2228.
24. A. R. Djordjević, M. B. Baždar, R. F. Harrington, and T. K. Sarkar, LINPAR for windows: matrix parameters for multiconductor transmission lines, Version 2.0 Software and User's Manual, Artech House, Norwood, MA, 1999.

25. Microwave Office 8.00, Applied Wave Research, 2008.
26. A. R. Djordjević, SPICE-compatible models for multiconductor transmission lines in Laplace-Transform domain, IEEE Trans Microwave Theory Tech 45 (1997), (Part I), 569–579.
27. A. R. Djordjević, R. M. Biljić, V. D. Likar-Smiljanić, and T. K. Sarkar, Wideband frequency-domain characterization of FR-4 and time-domain causality, IEEE Trans Electromagn Compat 43 (2001), 662–667.
28. IE3D v9, Zeland Software, Inc. Fremont, CA. 2003. Available at: http://www.zeland.com.
29. WIPL-D Pro 8.0, 3D Electromagnetic Solver. Available at: http://www.wipl-d.com.

SMALL SQUARE SLOT ANTENNA WITH DUAL BAND-NOTCH FUNCTION BY USING INVERTED T-SHAPED RING CONDUCTOR-BACKED PLANE

Nasser Ojaroudi[1] and Mohammad Ojaroudi[2]
[1] Department of Electrical Engineering, Ardabil Branch, Islamic Azad University, Ardabil, Iran
[2] Young Research Club, Ardabil Branch, Islamic Azad University, Ardabil, Iran; Corresponding author: m.ojaroudi@iauardabil.ac.ir

ABSTRACT: *In this article, a novel method for designing a new slot antenna with dual band-notch characteristic for ultra-wideband applications has been presented. By inserting a coupled inverted T-shaped ring strip on the other side of the substrate, a dual band-notch function generated, also additional resonance is excited and hence much wider impedance bandwidth can be produced, especially at the higher band. The measured results reveal that the presented dual band-notch slot antenna offers a wide bandwidth with two notched bands, covering all the 5.2/5.8-GHz wireless local area network, 3.5/5.5-GHz WiMAX, and 4-GHz C bands. The designed antenna has a small size of 20 × 20 mm². Good return loss and radiation pattern characteristics are obtained in the frequency band of interest.* © 2012 Wiley Periodicals, Inc. Microwave Opt Technol Lett 54:2267–2270, 2012; View this article online at wileyonlinelibrary.com. DOI 10.1002/mop.27057

1. INTRODUCTION

Ultrawideband (UWB) systems and applications developed rapidly in recent years. It's plenty of advantages, such as simple structure, small size, and low cost due to have received increased attention especially microstrip antenna are extremely attractive to be used in emerging UWB applications, and growing research activity is being focused on them. Consequently, a number of planar microstrip antenna with different geometries have been experimentally characterized [1–4].

The frequency range for UWB systems between 3.1 and 10.6 GHz will cause interference to the existing wireless communication systems, such as, the wireless local area network (WLAN) for IEEE 802.11a operating in 5.15–5.35 GHz and 5.725–5.825 GHz bands, WiMAX (3.3–3.6 GHz and C-band (3.7–4.2 GHz), so the UWB antenna with a single and dual-bandstop performance is required [5, 6].

A simple method for designing a novel and compact microstrip-fed slot antenna with multiresonance performance and dual-band-notch characteristics for UWB applications has been presented. In the proposed structure, by adding an inverted
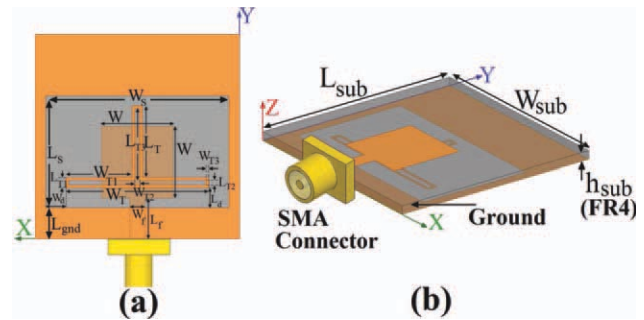
Figure 1 Geometry of proposed square slot antenna with an inverted T-shaped ring conductor backed plane, (a) bottom view, (b) side view. [Color figure can be viewed in the online issue, which is available at wileyonlinelibrary.com]

T-shaped ring conductor-backed plane, dual band-notch characteristic is obtained, also additional resonance is excited and the bandwidth is improved that achieves a fractional bandwidth with multiresonance performance of more than 135% (3.1–5.83 GHz). Simulated and measured results are presented to validate the usefulness of the proposed antenna structure for UWB applications.

2. ANTENNA DESIGN

The presented small square slot antenna fed by a 50-Ω microstrip line is shown in Figure 1, which is printed on an FR4 substrate of thickness 0.8 mm, permittivity 4.4, and loss tangent 0.018. The basic slot antenna structure consists of a square radiating stub, a feed line, and a ground plane. The square patch has a width W. The patch is connected to a feed line of width W_f and length L_f. On the other side of the substrate, a conducting ground plane with a rectangular slot and a coupled inverted T-shaped ring strip is placed. The proposed antenna is connected to a 50-Ω SMA connector for signal transmission.

On the basis of the electromagnetic coupling theory, the conductor-backed plane perturbs the resonant response and also acts as a parasitic half-wave resonant structure electrically coupled to the square radiating stub [5]. In addition, the conductor-backed plane is playing an important role in the broadband characteristics of this antenna, because it can adjust the electromagnetic coupling effects between the patch and the ground plane, and improves its impedance bandwidth without any cost of size or expense. This phenomenon occurs because, with the use of a conductor-backed plane structure, additional coupling is introduced between the bottom edge of the square patch and the ground plane [6].

The optimized values of proposed antenna design parameters are as follows: $W_{sub} = 20$ mm, $L_{sub} = 20$ mm, $h_{sub} = 0.8$ mm, $W_f = 1.5$ mm, $L_f = 3.5$ mm, $W = 10$ mm, $W_t = 14$ mm, $L_t = 8.75$ mm, $W_{t1} = 6.75$ mm, $L_{t1} = 0.5$ mm, $W_{t2} = 0.2$ mm, $L_{t2} = 0.5$ mm, $W_{t3} = 0.15$ mm, $L_{t3} = 8.6$ mm, $W_d = 2$ mm, $L_d = 1.75$ mm, $W_{P3} = 3$ mm, $L_{P3} =$ mm, and $L_{gnd} = 3.5$ mm.

3. RESULTS AND DISCUSSION

The proposed microstrip-fed slot antenna with various design parameters were constructed, and the numerical and experimental results of the input impedance and radiation characteristics are presented and discussed. The Ansoft simulation software high-frequency structure simulator (HFSS) [7] is used to optimize the design and agreement between the simulation and measurement is obtained.